UNDERSTANDING SPECTRAL VARIABILITY AND TIME LAGS IN ACCRETING BLACK HOLES

Juri Poutanen [1]

[1] *Stockholm Observatory, SE-133 36 Saltsjöbaden, Sweden*

ABSTRACT

I review the temporal/spectral data of accreting black hole sources paying most attention to the properties of the temporal variability such as photon energy dependent auto- and cross-correlation functions, average shot profiles and hardness ratios, and the Fourier frequency dependent time/phase lags. These statistics characterize spectral changes at short time scales that are otherwise impossible to study by direct spectral analysis. The data provide strong constraints on the theoretical models for X-ray production in accreting black holes. Models for the spectral variability of the Comptonized component are briefly reviewed. It is also shown that Compton reflection can have significant impact on the observed temporal characteristics.

INTRODUCTION

Accreting Galactic black holes (GBHs) in X-ray binaries and supermassive black holes in active galactic nuclei (AGNs) in the centers of Seyfert galaxies show similar X-ray/γ-ray spectra. In the X-ray band, spectra can be described as a cutoff power-law with a Compton reflection bump atop of that (see Fig. 1a). All GBHs in their hard states that were observed with sufficient sensitivity above 100 keV (e.g. by Sigma instrument onboard the *Granat Observatory* and OSSE instrument onboard the *Compton Gamma-Ray Observatory*) show a sharp cutoff at about 100 keV (e.g. Gilfanov et al. 1995; Grebenev et al. 1993, 1997; Grove et al. 1998a; Gierliński et al. 1997; Zdziarski et al. 1997; Zdziarski 1999). Similar cutoff is observed in the spectra of bright Seyfert galaxies such as NGC 4151 and NGC 5548 (Zdziarski, Johnson, & Magdziarz 1996; Magdziarz et al. 1998), and in the composite spectrum of a number of weaker Seyferts (Zdziarski, Poutanen, & Johnson 2000).

It is broadly accepted that the only mechanism capable of producing a power-law spectrum with the cutoff at a similar energy in objects that differ by orders of magnitude in luminosity, size, and a BH mass is thermal Comptonization (e.g. Sunyaev & Titarchuk 1980). The observed spectra are produced in a cloud of hot electrons with the temperature $kT_e \sim 50 - 100$ keV and Thomson optical depth $\tau_{\rm T} \sim 1$ (for a review see Zdziarski et al. 1997). Only in the brightest objects such as Cyg X-1 deviations from thermal Comptonization model at high energies are statistically significant (McConnell et al. 2000b). An excess of the emission above > 1 MeV (see Fig. 1b) is a possible signature of non-thermal electrons in the source (Li, Kusunose, & Liang 1996; Poutanen 1998). The X/γ-ray spectra of GBHs in the soft state are dominated by a black body type emission at ~ 1 keV with a power-law tail extending at least up to 400-800 keV (Grove et al. 1998a; Gierliński et al. 1999) or maybe even up to 10 MeV (McConnell et al. 2000a). The tail is most probably produced by Comptonization in non-thermal plasmas (Poutanen & Coppi 1998; Gierliński et al. 1999; for reviews see Poutanen 1998; Coppi 1999).

All spectral models (particularly those incorporated into XSPEC) are designed to fit the time averaged spectra. However, it is known that black holes show spectral variability reflected in time lags, asymmetries of the cross-correlations function, and changes of the hardness ratio. On longer time scales (minutes-hours for GBHs, days for AGNs), spectral changes can be tracked directly by fitting the spectrum averaged over that time interval and following the changes in the best fit parameters. However, it is not possible to determine directly how the spectrum changes on very short time scales corresponding to the characteristic time scales close to the black hole. One can do it only in a statistical sense, i.e. by analyzing different statistics of the

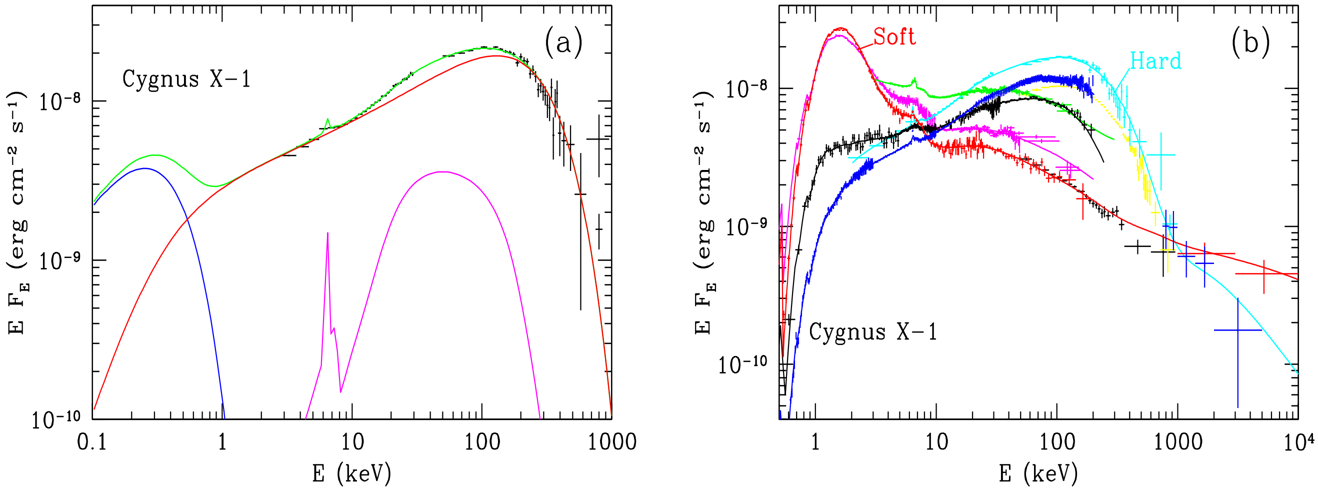

Fig. 1. (a) Cygnus X-1 in the hard state (data from Gierliński et al. 1997). Spectrum can be decomposed into several components: thermal Comptonization, Compton reflection, and a soft excess (modeled here as a ~ 0.1 keV black body). (b) Spectral states of Cygnus X-1. Courtesy of A. A. Zdziarski.

temporal-spectral variability, such as auto- and cross-correlation functions (ACF/CCF) in different energy channels, power-density spectra (PDS), cross-spectra, phase/time lags, coherence function, etc. that contain important information about the physical processes responsible for X-ray production.

Ideally, any model describing the spectral properties of black holes should also describe their temporal characteristics. In this review, I will first discuss the data obtain by time domain analysis. Then the results obtained via Fourier analysis are presented. Finally, I will review models proposed to describe temporal and spectral properties.

VARIABILITY IN THE TIME DOMAIN

Auto- and cross-correlation functions of GBHs

Time domain techniques were used at the very early days of the X-ray astronomy. In the 70-ies, the auto- and cross-correlation function of Cyg X-1 were obtained (Weisskopf, Kahn, & Sutherland 1975; Sutherland, Weisskopf, & Kahn 1978; Priedhorsky et al. 1979; Nolan et al. 1981). The asymmetry of the CCF of Cygnus X-1 was discovered in ~ 150 sec observations by Priedhorsky et al. (1979) and Nolan et al. (1981). They showed that the CCF peaks at a lag $\lesssim 10 - 40$ ms. Using the *EXOSAT* data, Page (1985) confirmed these results and claimed a ~ 6 ms shift of the peak of the CCF between the 5-14 keV and the 2-5 keV bands. For many years, the time domain analysis was not applied to GBHs despite immense advances in temporal resolution, photon statistics, and duration of observations. Aside from attempts to model individual shots (Lochner, Swank, & Szymkowiak 1991; Negoro et al. 1994; Feng et al. 1999), recent analyses have concentrated on Fourier domain techniques.

Recent *RXTE* observations (Maccarone, Coppi, & Poutanen 2000) clearly show asymmetries of the CCFs, which, however, peak within ~ 1 ms from zero lag (see Fig. 2). This suggests that the relation between the variation in the two bands are not simply a time delay. The rising part of the CCF (soft lags) becomes narrower with energy substantially faster than the decaying part (hard lags). This is in qualitative agreement with the results of Priedhorsky et al. (1979) and Nolan et al. (1981). The CCFs reach values very close to unity, showing that the signal at all the energies is extremely well synchronized. Asymmetry is also observed in the *RXTE* data of GX 339-4, where the CCFs are offset by $\lesssim 5$ ms from zero (using the 2-5 and 10-40 keV bands, Smith & Liang 1999). The CCFs of AGNs also display similar properties (e.g., Papadakis & Lawrence 1995; Lee et al. 2000).

Maccarone et al. (2000) presented also the ACFs of Cygnus X-1 which are shown in Figures 2 and 3a. The width of the ACF decreases with photon energy approximately as $\propto E^{-0.2}$ at lags smaller than ~ 0.3 sec. (At larger lags the ACFs at different energies are not self-similar.) This strongly constrains the origin of the spectral variability, since it requires that the pulses producing the variability last longer at low energies than at higher energies.

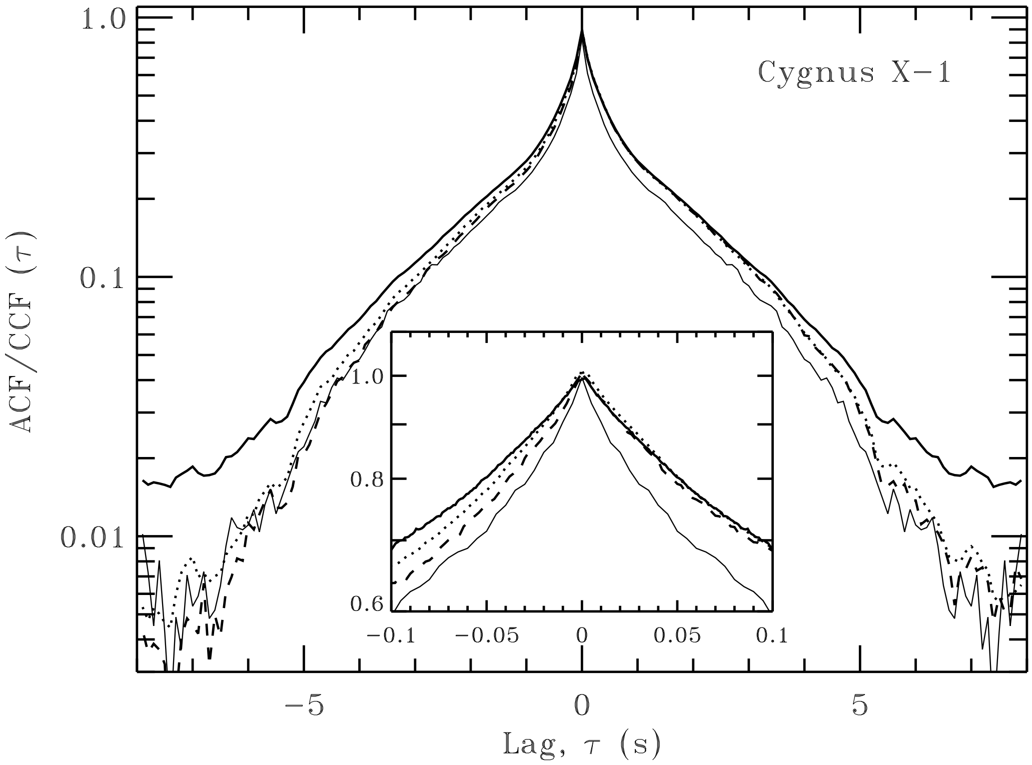

Fig. 2. The auto- and cross-correlation functions of Cygnus X-1 observed in December 1997. Solid curves show the ACFs for the 2-5 keV energy band (thick curves) and the 24-40 keV band (thin curves). Dotted curves show the CCF between the 8-13 keV band and the 2-5 keV band, and dashed curves represent the CCF for the 24-40 keV band vs the 2-5 keV band. The peaks all align at around zero lag. The higher energy curves are narrower. The CCFs are defined in such a way that the peak is expected to appear at a positive lag when hard photons are lagging the soft ones. From Maccarone, Coppi, & Poutanen (2000).

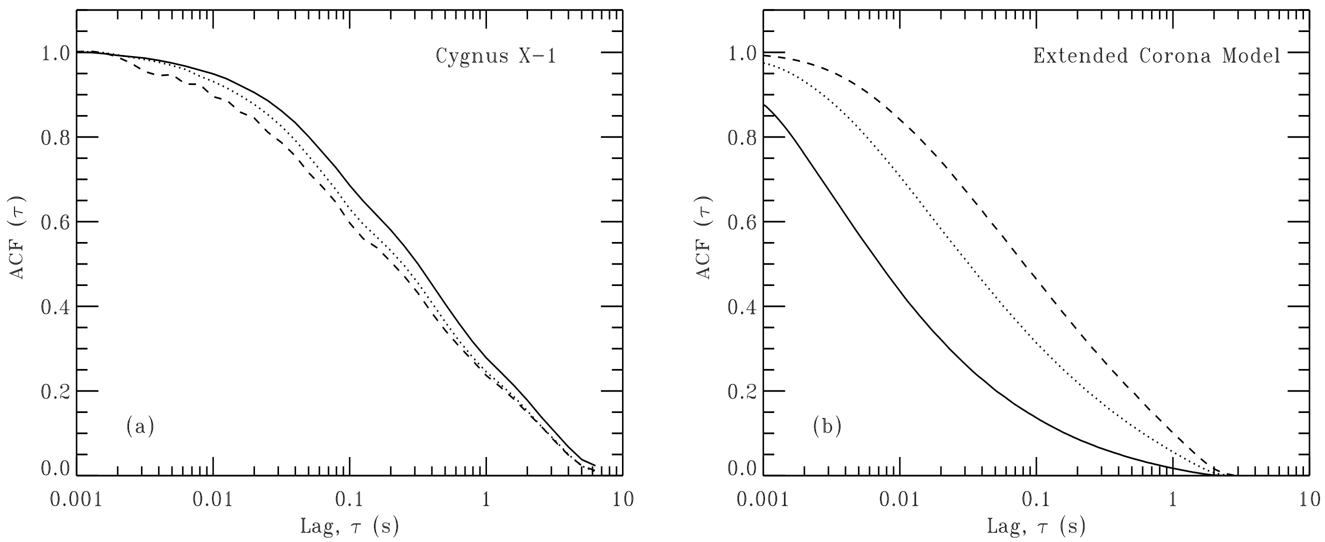

Fig. 3. The ACFs in the different energy bands. (a) The data for Cygnus X-1. Solid curves shows the ACF for the 2-5 keV energy band, dotted curve is for 8-13 keV band, and dashed for 24-40 keV band. (b) The prediction of the extended corona model (Kazanas et al. 1997; Hua et al. 1999). From Maccarone et al. (2000).

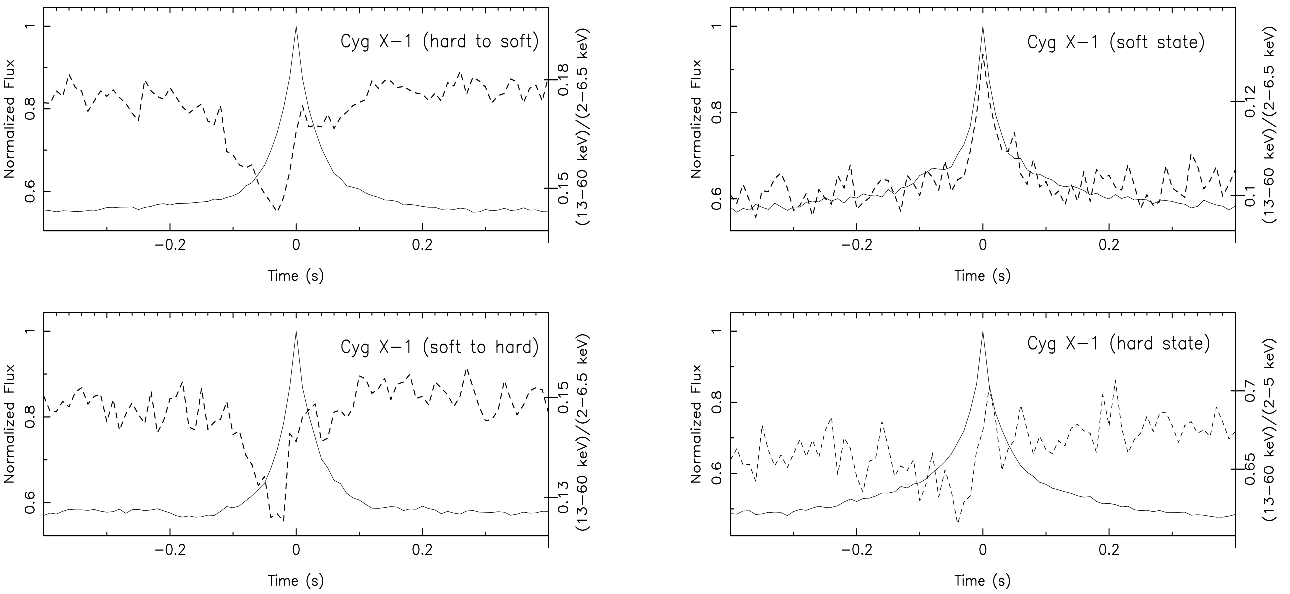

Fig. 4. Peak aligned average shots in Cygnus X-1 and their hardness ratios. In different spectral states the hardness (dashed curves) varies differently along the shot light curve (solid curves). From Li, Feng, & Chen (1999).

Average Peak Aligned Shots

A different approach to analyzing variability in the time domain was taken by Negoro, Miyamoto, & Kitamoto (1994), Feng, Li, & Chen (1999), and Li, Feng, & Chen (1999). They constructed the average peak aligned profiles of the shots in Cyg X-1 at different energies (see Fig. 4). This procedure is rather similar to that used in the analysis of the light curves of gamma-ray bursts (see e.g. Stern, Poutanen, & Svensson 1997, 1999). In spite of the fact that definition of a shot itself is rather ad hoc, this procedure provides some insight into spectral variability during bright emission episods. In the hard state, the shot becomes first softer, and then, just after the peak, harder than the average emission (Negoro et al. 1994). In the soft state, shots are harder, and in the transition states softer than the time average emission.

The behavior in the soft state is easy to understand. It is known that the disk (black body like) emission dominating the 2-6 keV energy band does not vary much, while the Comptonized hard (power-law like) tail dominating energy band above 13 keV is strongly variable (Churazov, Gilfanov, & Revnivtsev 2001). An increase in flux ("shot") implies an increase in the normalization of the hard tail and larger hardness ratio. It would be of interest to see, however, how the hardness in the energy bands above ~ 10 keV varies. This would provide important information about spectral variability of the hard tail.

The transition state of Cyg X-1 is characterized by strong QPO type oscillations at $\sim 1 - 10$ Hz. The softening of the spectrum during increase of the count rate can be a result of those oscillations that cause changes in the geometry of the emission region, e.g. by changing the overlap between hot inner disk and cold outer disk (see Fig. 5a). Such changes can be similar to the long term changes characterizing spectral transitions (Poutanen, Krolik, & Ryde 1997; Esin et al. 1998; see Fig. 1b). More overlap increase Compton cooling by soft photons from the cold disk, causing temperature of the Comptonizing region to decrease and softening the spectrum. In the magnetic flare model with plasma ejection (Beloborodov 1999a,b), similar spectral evolution occurs if the plasma ejection velocity is variable. Smaller velocity means more feedback from the cold disk, more soft seed photons coming to the emission region, and softer spectrum. One should caution the reader that at energies above 13 keV most of the variability power emerges at ~ 10 Hz QPO and the average shot techniques does not say almost anything about spectral evolution at these time scales.

The hard-state spectral evolution is the most complicated one. The observed behavior could be reproduced by a magnetic flare model (Poutanen & Fabian 1999) where increasing separation of the flare from the underlying cold disk produces changes in the feedback and corresponding spectral evolution (Fig. 5b).

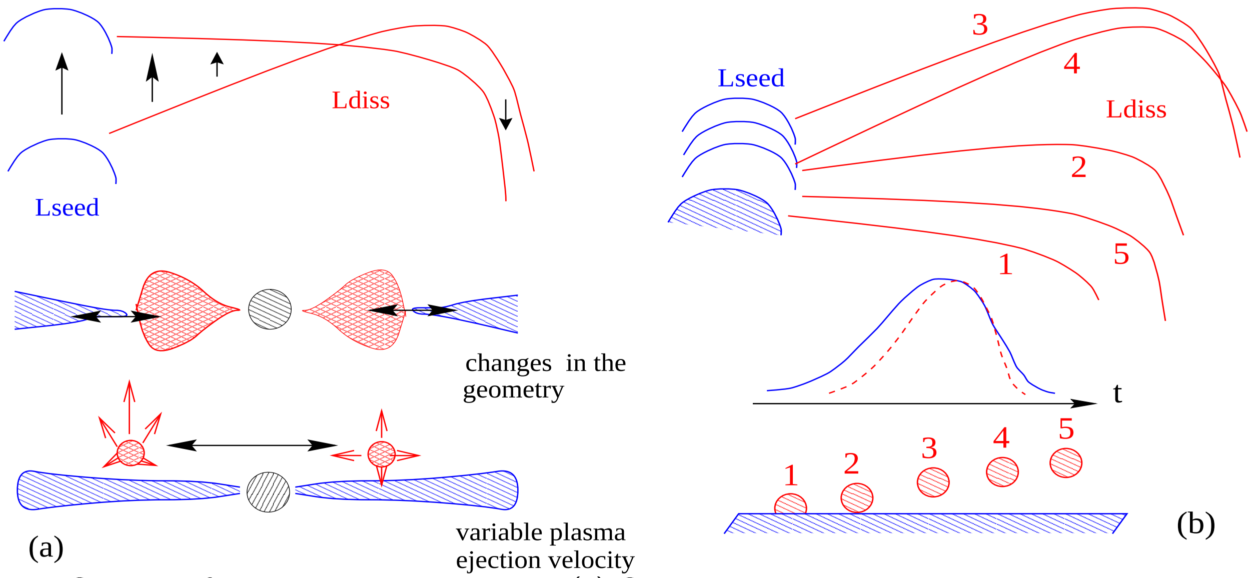

Fig. 5. Cartoons of the variability mechanisms. (a) Changes in the geometry or ejection velocity cause corresponding changes in the seed soft photon luminosity entering the hot Comptonizing plasma cloud. The spectrum pivots if the heating rate in the hot cloud stays constant. Such variability could be responsible for the observed spectral changes in the transition state. (b) Spectral evolution of the magnetic flare (Poutanen & Fabian 1999). Movement of the X-ray emitting cloud from the underlying disk changes the feedback. This in turn causes soft-hard-soft evolution of the flare spectrum that satisfies observational constraints in the hard state of Cyg X-1. If the energy dissipation rises slower than it decays, shots at higher energy (dashed curve) are narrower than low energy shots (solid curve) satisfying constraints from the ACF (see Fig. 3).

FOURIER ANALYSIS AND TIME LAGS

In spite of the fact that Fourier domain functions contain, in principle, the same information as their time domain companions, they highlight different information which can be used to constrain the models. During last decade a number of authors studied Fourier-frequency–dependent time lags between photons in different energy channels for many accreting black holes and neutron stars (see e.g. Miyamoto et al. 1988, 1992; Cui et al. 1997; Nowak et al. 1999a,b; and Poutanen 2001 for a recent review). By computing the cross-spectrum $C(f) \equiv \tilde{S}^*(f)\tilde{H}(f)$ (here $\tilde{S}(f)$ and $\tilde{H}(f)$ are the Fourier transforms of the light curves in the soft and hard energy channels, respectively, and f is the Fourier frequency), the phase lag, $\delta\phi(f) \equiv \arg[C(f)]$, can be obtained. The time lag is then, $\delta t(f) \equiv \delta\phi(f)/(2\pi f)$. The lags are positive when hard photons are lagging the soft ones (hard lags).

There are a few important facts to notice. First, time lags are normally hard (except when strong quasi-periodic oscillations are present in the data, see e.g. Cui 1999; Reig et al. 2000 for the case of GRS 1915+105, and Cui, Zhang, & Chen 2000 for the case of XTE 1550-564). Second, they depend approximately logarithmically on photon energy, i.e. $\delta t(f) \propto \ln(E_h/E_s)$, where E_h and E_s and the energies of the "hard" and "soft" channel (Miyamoto et al. 1988; Nowak et al. 1999a). Third, time lags depend on the Fourier frequency in a quite complicated fashion (see Fig. 6a). At high frequencies, $\delta t(f) \propto 1/f$. It is also interesting to note that in Cyg X-1 as well as in GX 339-4 (Nowak et al. 1999b) and GRO J0422+32 (Grove et al. 1998b) there is a break in the time-lag spectrum at $f \sim 0.1 - 0.5$ Hz.

MODELS FOR SPECTRAL VARIABILITY AND TIME LAGS

Models that were proposed to explain temporal properties of accreting black holes can be generally divided into a few groups. Phenomenological shot noise models belong to the first group. Here, any dependence of shots on energy is just postulated. Such models can successfully reproduce energy dependence of ACF/CCFs, time lags, PDS, coherence function, etc. (see e.g. Miyamoto & Kitamoto 1989; Poutanen 2001; and Fig. 6). However, they leave unanswered the question of the origin of spectral variability. In another class of models, the variability is related to the Comptonized component. Here either seed soft photons are considered as the source of variability with constant properties of a hot Comptonizing cloud (Kazanas, Hua, & Titarchuk

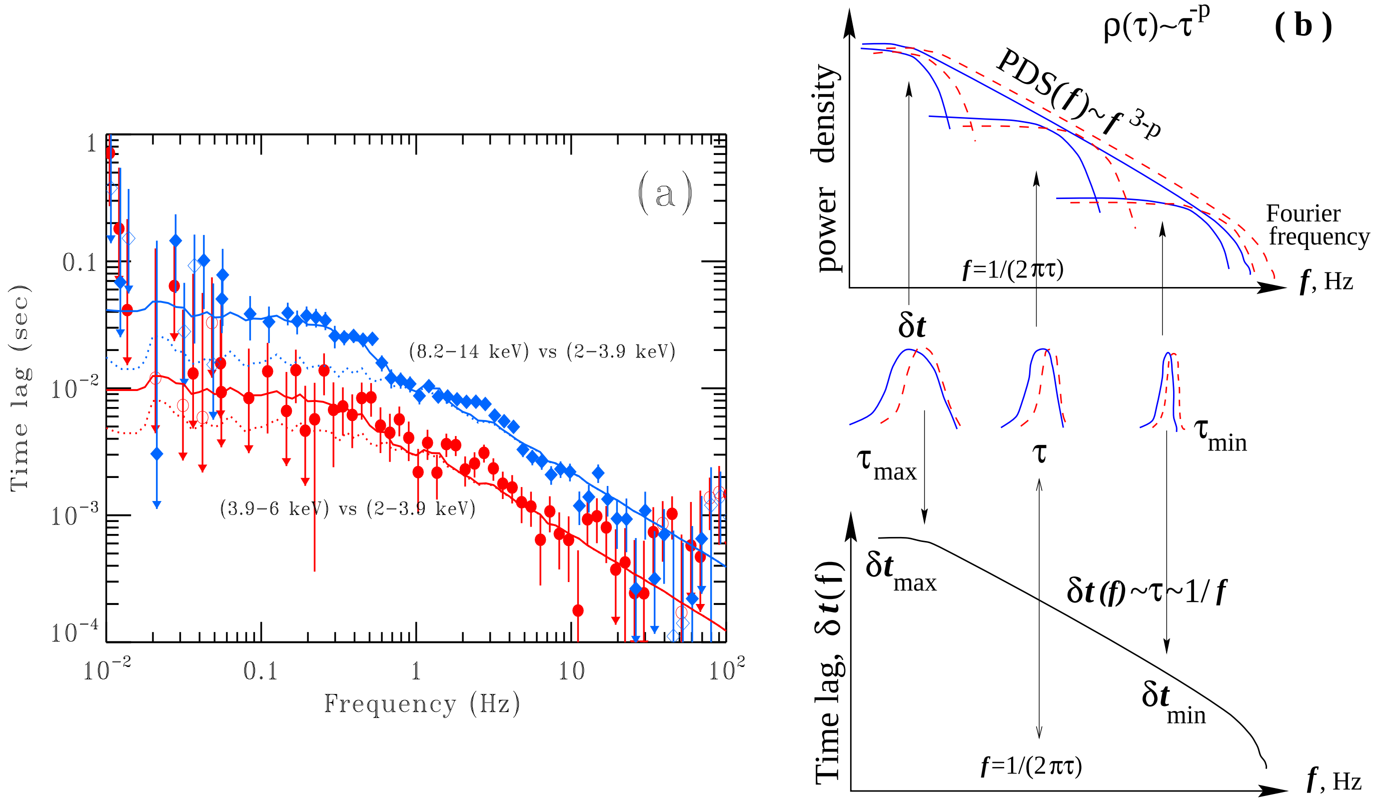

Fig. 6. (a) Time lags in the hard state of Cyg X-1 (Nowak et al. 1999a; Pottschmidt et al. 2000). Dotted curves show the modified shot noise model with time scales between $\tau_{\rm min} = 1$ ms and $\tau_{\rm max} = 0.2$ s (Poutanen & Fabian 1999). The shots at higher energies are delayed as shown on the right panel (see also Fig. 5b). A fraction of hard photons can be delayed due to Compton reflection in the outer part of the disk, time lags increase then at low Fourier frequencies. The total lags are shown by solid curves.
(b) Time lags and PDS for a modified shot noise model. Shots at softer energies are shown by solid curves, and at higher energies by dashed curves. For a power-law distribution of time scales $\rho(\tau) \propto \tau^{-p}$, the resulting PDS is a power-law. If the delay between the shots at different energies is a constant fraction of τ, the resulting time lags are $\delta t(f) \propto 1/f$.

1997; Böttcher & Liang 1998; Hua, Kazanas, & Cui 1999; Böttcher & Liang 1999), or the hot cloud itself is responsible for variability due to changes of the energy dissipation rate (Poutanen & Fabian 1999; Malzac & Jourdain 2000) or propagation of waves (Kato 1989; Misra 2000). The third group considers the impact of Compton reflection from the accretion disk (e.g. Vikhlinin 2000; Poutanen, in preparation). Below, I briefly review the proposed models and constraints on the models from observations.

Shot Noise Models

One can attempt to interpret the observed ACFs, CCFs and the average shot profiles in terms of a simple shot noise model (Terrell 1972). Since the CCFs peak at a lag $\lesssim 2$ ms, the shots at different energies also should reach maxima within 2 ms from each other. The energy dependence of the ACF requires the shots at higher energies to be shorter. Based on the shape of the CCF, Maccarone et al. (2000) (see also Miyamoto & Kitamoto 1989) also argued that shot's rise time scale decreases at high energies and the decay times at different energies are very close to one another or are much smaller than the rise time scales. The energy dependence of the rise time then produces the hard time lags and the asymmetry of the CCF.

For a broad distribution of shot time scales, τ, one comes to the modified shot noise models (see, e.g., Lochner et al. 1991). The properties of the shot behavior at different energies can be summarized as follows. In order to achieve high values of the CCFs, the shots at different energies should be perfectly synchronized. The observed hard lags can be produced only if hard shots are delayed relative to the soft ones. This delay is approximately a constant fraction of τ (see Fig. 6) and should grow as $\ln(E_h/E_s)$ with energy, since the observed time lags are approximately inversely proportional to the Fourier frequency, $\delta t(f) \propto f^{-1}$, and grow logarithmically with energy. And finally, since ACF's width decreases with energy, hard shots should be narrower than soft shots.

Comptonization Models

In the process of Comptonization, soft photons are scattered by hot electrons and gain energy. Harder photons are produced in a larger number of scattering, and they spend on average more time in the hot cloud. Therefore, hard photons lag behind soft photons. The characteristic delay between photons of energies E_h and E_s for a cloud of size R and temperature $\Theta = kT_e/m_e c^2$ is (Sunyaev & Titarchuk 1980; Payne 1980)

$$t_c = \frac{R}{c(1+\tau_{\rm T})} \frac{\ln(E_h/E_s)}{\ln[1+4\Theta(1+4\Theta)]}. \tag{1}$$

Comptonization in a uniform electron cloud produces frequency independent time lags (Miyamoto et al. 1988). In order to reproduce large values of lags, their f^{-1} dependence, and their logarithmic dependence on energy, Kazanas et al. (1997) proposed an extended corona model with a r^{-1} radial density distribution and a few light seconds in size. The long lags at low Fourier frequencies are attributed to photons traveling over large radii, while the shorter time lags at high frequencies are produced in the central small core of the cloud. The model predicts reduced variability of the higher energy photons at high frequencies. On the other hand, the PDS of Cyg X-1 hardens with energy (Nowak et al. 1999a), i.e. the high energy photons are more variable. Using time domain analysis, Maccarone et al. (2000) showed that the extended corona model predicts the ACF's width to grow with energy (the 30 keV ACF is ten times broader than the 3 keV ACF), while the observations show that the ACF becomes narrower with energy (see Fig. 3). They concluded that any model where the time lags are the result of light travel delays can be ruled out. One should note that this, of course, does not rule out Comptonization as a mechanism for the X-ray production.

Magnetic Flares

The observed spectrum can be generated by magnetic flares on the surface of the cold accretion disk (see e.g. Haardt, Maraschi, & Ghisellini 1994; Stern et al. 1995; Poutanen & Svensson 1996; Beloborodov 1999a,b). The magnetic fields amplified in the accretion disk and expelled from it due to the Parker instability elevate to the corona releasing magnetic energy and heating the corona. The flare time scales are probably of the order of the Keplerian time scale at a given distance from the central black hole. In the model by Poutanen & Fabian (1999), changes in the energy dissipation rate and in the geometry of the flare (e.g. the distance from the disk) produce soft-to-hard spectral evolution which is the cause of the hard time lags. A broad distribution of the flare time scale τ (as for a modified shot noise model) assures that the time lags are inversely proportional to the Fourier frequency $\delta t(f) \propto \tau \sim 1/(2\pi f)$ (see Fig. 6).

This model reproduces well the time lags observed in Cyg X-1. Energy dependence of the ACF/CCFs can be accounted for only if the energy dissipation rate in flares rises slower than it decays (Maccarone et al. 2000). When the flare time scale is comparable to the light emission region crossing time, R/c, the model predicts soft time lags at high frequencies $f \gtrsim 1/(20R/c)$ independently of the energy dissipation rate profile (Malzac & Jourdain 2000; see Fig. 7). This property can be used to put constraints on the size of the emission region.

Cold Blobs in Hot Disk

One of the viable model for the X-ray emission is the hot inner disk model (e.g. Esin et al. 1998). The soft photons can be produced by external cold disk or by cold blobs inside the hot material. Böttcher & Liang (1999) considered cold blobs drifting towards the black hole. When blobs enter the innermost hottest region of the disk the radiation was assumed to increase due to the influx of the soft seed photons. The overall spectrum then hardens. The spectral evolution results in hard time lags. The problem is that if the energy dissipation rate in the hot disk does not vary, then an increase of the soft photon flux would lead to a softer spectrum (not a harder one). In order to save the model, one has to assume that the inward drift of cool blobs is perfectly correlated with the increase of the energy dissipation in the hot disk. It remains to be seen whether such a requirement is physically realistic and the model can indeed fit the data.

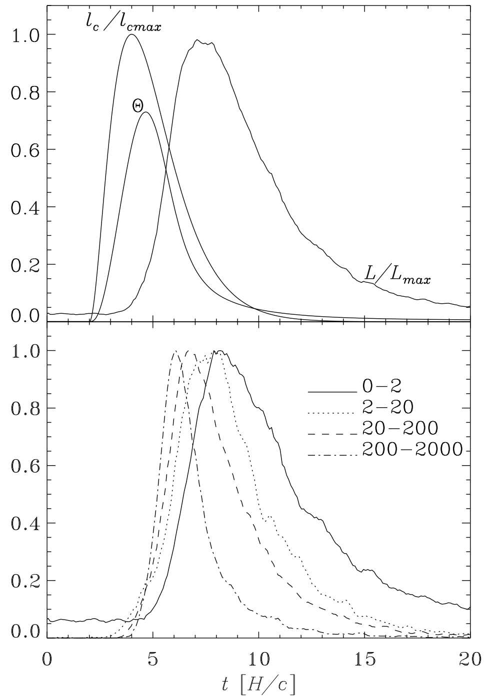

Fig. 7. Spectral evolution of a strong flare (in a slab-corona geometry). Upper panel shows the evolution of the dissipation rate l_c, electron temperature Θ, and the emitted luminosity L (for a constant $\tau_{\rm T} = 0.4$). Lower panel shows time evolution of the observed flux in different energy intervals. The time scale of the flare is about the slab light crossing time, H/c. The seed photon flux is dominated by reprocessed photons. In such conditions, the spectrum is hard in the beginning of the flare due to photon starvation (it takes a few H/c to produce soft photons). Spectrum softens in the end of the flare. Independently of the energy dissipation temporal evolution, softer photons escape on average after harder ones. Adapted from Malzac & Jourdain (2000).

Waves in the Disk

Several papers discussed models where hard time lags are produced by waves propagating through the accretion disk from the outer, cooler region to the inner, hotter region (e.g., Miyamoto et al. 1988; Kato 1989; Nowak et al. 1999c). Frequency dependent time lags appear due to dispersion of wave velocities. Most of the models do not however specify the radiative processes responsible for the X-ray emission. Recently, Misra (2000) proposed that Comptonization in a"transition disk" with varying temperature could be responsible for that emission. In that model, emission at 30 keV is delayed by ~ 0.015 s from the peak at 3 keV. Maccarone et al. (2000) argued that, in such a case, the CCF between the 30 keV and 3 keV photons would peak at that lag strongly contradicting the data for Cyg X-1. Since the signal at different energies is produced in physically separated regions, it is very difficult to understand how it is possible to keep very high coherence of the signals at different energies (see e.g. Nowak et al. 1999a).

Impact of Compton Reflection on Temporal Characteristics

Observations show that accretion disks in X-ray binaries are geometrically thick at the outer edge (White & Holt 1982; Mason & Cordova 1982; Vrtilek et al. 1990; Hynes et al. 1998; see Verbunt 1999 for a recent review). The height-to-radius ratio, H/R, at the outer edge of the disk can be as large as 0.15-0.5. This is much larger than is predicted by the standard accretion disk theory. A large fraction of the X-rays from the central source is intercepted by the disk and some are reflected. These (Compton) reflected photons are significantly delayed relative to the direct emission. Since Compton reflection spectrum is very hard, at higher energies a larger fraction of photons is delayed. This produces hard time lags (see below).

The reflection spectrum as a function of time, $I_r(E,t)$, can be represented as a convolution of the direct/intrinsic spectrum, $I(E,t)$, with the transfer function, $T(t)$ (normalized to the total observed amplitude of reflection), describing the time delay and Green's function, $G(E,E')$, describing the process of Compton downscattering and photoelectric absorption,

$$I_r(E,t) = \int_{-\infty}^{t} T(t-t')dt' \int_{E}^{\infty} G(E,E')I(E',t')dE'. \tag{2}$$

This equation can be simplified if one neglects the process of Compton down-scattering (i.e. for low energy X-ray photons, $E \lesssim 10$ keV), and approximate the redistribution function by a delta-function, $G(E,E') = a(E)\delta(E-E')$ (here $a(E)$ is the reflection albedo). Then

$$I_r(E,t) = a(E) \int_{-\infty}^{t} T(t-t')I(E,t')dt'. \tag{3}$$

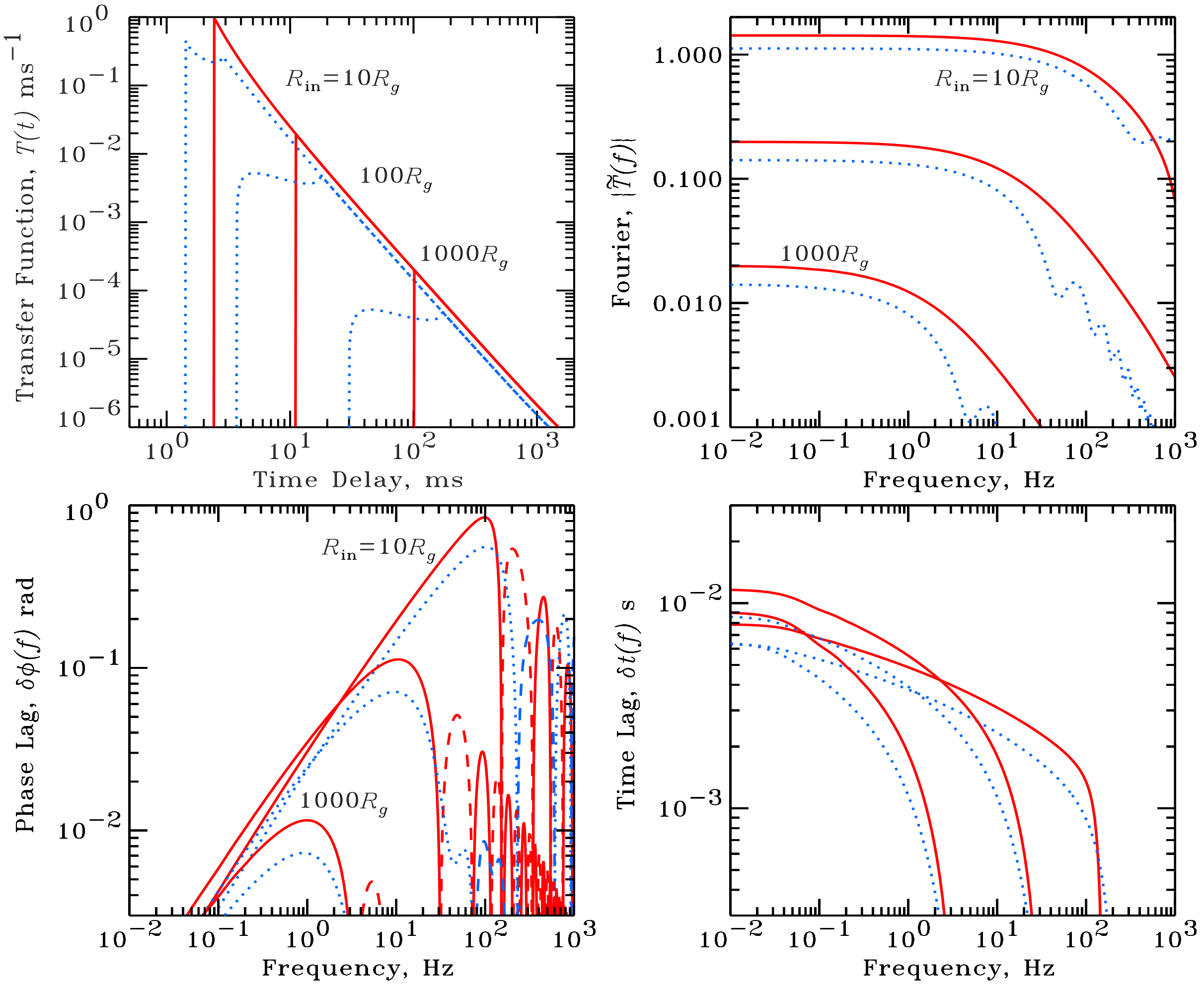

Fig. 8. Response and time lags produced by reflection off the flat disk with the central hole of different radii $R_{\rm in}$. Solid curves are for inclinations $i=0^{\rm o}$ and dotted curves are for $i=45^{\rm o}$. Dashed curves give negative lags. Isotropic flare is at the center at elevation $h_{\rm fl}=10R_g$. Time and frequency units correspond to the $10M_{\odot}$ black hole ($R_g=2GM/c^2=30$ km). Albedos $a_s=0, a_h=1$ are assumed. The angular distribution of reflection is $2\cos i$.

Let us consider light curves in the two energy bands which are composed of the direct radiation from the X-ray source plus the reflected radiation:

$$S(t)=S_d(t)+a_s\int_{-\infty}^{t}T(t-t')S(t')dt', \quad H(t)=H_d(t)+a_h\int_{-\infty}^{t}T(t-t')H(t')dt'. \tag{4}$$

Here a_s and a_h are the respective X-ray albedos. The Fourier transforms are:

$$\tilde{S}(f)=\tilde{S}_d(f)[1+a_s\tilde{T}(f)], \quad \tilde{H}(f)=\tilde{H}_d(f)[1+a_h\tilde{T}(f)]. \tag{5}$$

The cross-spectrum

$$\tilde{S}^*(f)\tilde{H}(f)=\tilde{S}_d^*(f)\tilde{H}_d(f)\left[1+a_s a_h|\tilde{T}(f)|^2+a_s\tilde{T}^*(f)+a_h\tilde{T}(f)\right]=|C_d(f)|e^{i\delta\varphi_d(f)}|C_r(f)|e^{i\delta\varphi_r(f)}, \tag{6}$$

where $C_d(f)$ and $\delta\varphi_d(f)$ are the cross-spectrum and the phase lag of the direct radiation. The reflection introduces into the signal an additional phase lag:

$$\tan\delta\varphi_r(f)=(a_h-a_s)\Im\tilde{T}(f)\Big/\left[1+(a_s+a_h)\Re\tilde{T}(f)+a_s a_h|\tilde{T}(f)|^2\right]. \tag{7}$$

For illustration, let us consider $a_s\ll 1$ (i.e. $E_s\lesssim 2$ keV), and specify a simple exponential transfer function, $T(t)=r_1\exp\{-(t-\tau_1)/\tau_1\}/\tau_1$ for $t>\tau_1$. After trivial calculations one gets:

$$\tan\delta\varphi_r(f)=a_h r_1(x\cos x+\sin x)\Big/\left[1+x^2+a_h r_1(\cos x - x\sin x)\right], \quad x=2\pi f\tau_1. \tag{8}$$

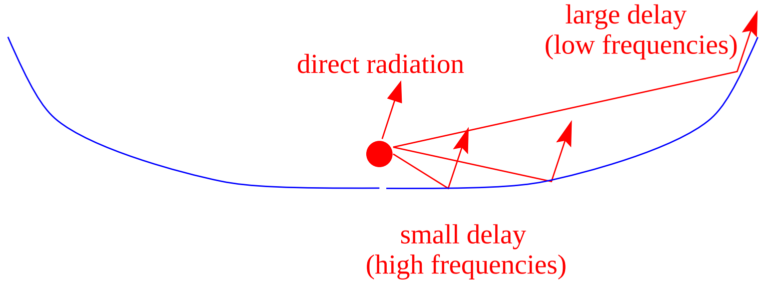

Fig. 9. Cartoon of the reflection from flared disk.

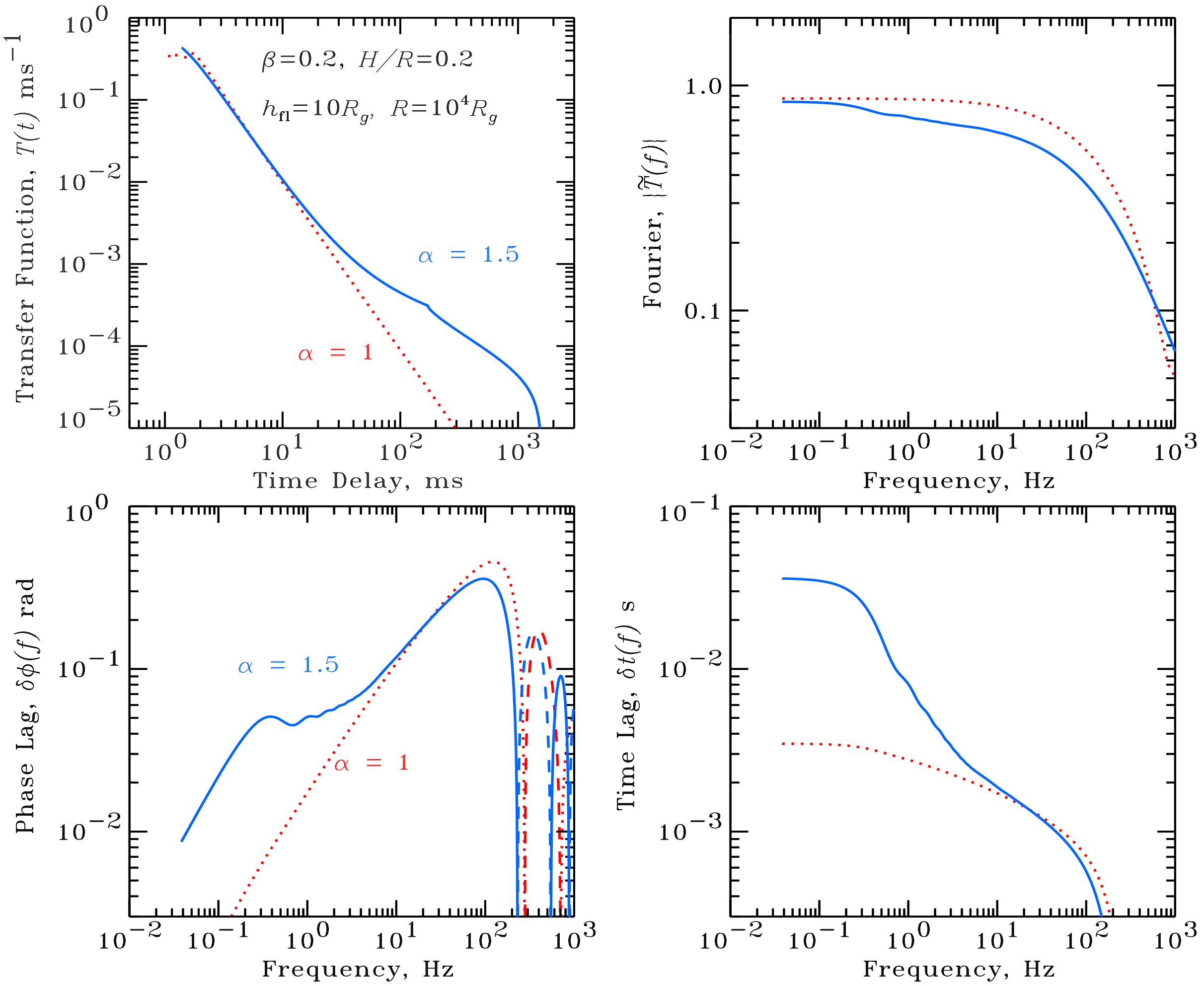

Fig. 10. Response of the flared disk and time lags. Flare is at the center at elevation $h_{\rm fl} = 10R_g = 300$ km (here it is assumed that the inner disk radius is 0); the size of the disk $R = 10^4 R_g = 1$ light sec; height to radius ratio of the disk $H/R = 0.2$; bulk velocity of the plasma $\beta = v/c = 0.2$ and inclination $i = 45^{\rm o}$. Height of the disk scales with radius as $h(r) \propto r^{\alpha}$. Solid curves correspond to $\alpha = 1.5$ and dotted curves to $\alpha = 1$. Dashed curves give negative lags.

The phase lag grows as $\delta\varphi_r(f) \approx 2a_h r_1 x/(1 + a_h r_1)$ for $x \ll 1$, and reaches the maximum $\tan\varphi_{r,\max,1} \approx 0.7a_h r_1/(1-0.15a_h r_1)$ at $x \approx 1$. One should note that for small $a_h r_1$, the energy dependence of the phase lag is exactly the same as that for the albedo a_h. If the transfer function is a sum of two exponentials described by τ_1, r_1 and τ_2, r_2, respectively (let $\tau_1 \ll \tau_2$), the phase lag has two prominent maxima at $f_1 \sim 1/(2\pi\tau_1)$ and $f_2 \sim 1/(2\pi\tau_2)$. The value of the high frequency maximum at f_1 stays the same, while the new low frequency maximum is $\tan\varphi_{r,\max,2} \approx 0.7a_h r_2/[1 + a_h(r_1 - 0.15r_2)]$.

Let us consider a specific physical situation where the X-rays produced close to the black hole (e.g. the hot disk) are reflected from a flat cold disk of a varying inner radius, $R_{\rm in}$ (Poutanen et al. 1997; Esin et al. 1998). For simplicity, we consider a point source in the center at elevation, $h_{\rm fl}$. The transfer functions and time/phase lags are shown in Figure 8 (see also Gilfanov et al. 2000). An analytical expression for the transfer function can be easily obtained for the inclination $i = 0$, $T(t) = 2ch_{\rm fl}/(ct - h_{\rm fl})^2$, where $ct > h_{\rm fl} + \sqrt{h_{\rm fl}^2 + R_{\rm in}^2}$ (a $2\cos i$ dependence of the amplitude reflection on inclination is assumed). Reflection works as a low pass filter, therefore the time lags appear only at low frequencies. For small inner radius, $R_{\rm in} = 10R_g$, the amplitude of reflection is significant and the maximum phase lag corresponds to the light travel time from the flare to the cold disk edge. For larger $R_{\rm in}$, the reflection is small and the time lags do not grow in spite of the fact that the characteristic distance to the reflector increases.

An interesting change in the time lag behavior occurs when the disk is flared (see Fig. 9). Then the outer parts of the disk occupy a significant solid angle as viewed from an X-ray source in the center. The intercepted photons can be delayed by a few seconds (in GBHs). The X-rays emission regions (magnetic flares) can be elevated above the disk and distributed all over its central part. For simplicity, we consider a "filled" disk (i.e. zero inner radius) and a point source elevated by $h_{\rm fl} = 10R_g$ above the center of the disk. Any small offset from the disk axis is negligible (see e.g. Gilfanov et al. 2000). The response and the amplitude of time lags depend on the angular distribution of the direct radiation from the X-ray flare. If plasmas in flares has bulk motion away from the disk the radiation is beamed towards the observer reducing the apparent amplitude of reflection (and time lags). Non-zero bulk velocity is required to explain the hard X-ray spectra and small reflection observed in GBHs (Beloborodov 1999a,b; Malzac, Beloborodov, & Poutanen 2001). The response of the disk can be represented approximately as a sum of responses from an infinite plane and from the outer edge of the disk. The results then can easily be understood from a trivial example of two exponential transfer functions (see above). Numerically computed transfer functions and time lags are presented in Figure 10. For a $h(r) \propto r^{\alpha}$ profile of the disk, $\alpha > 1$ produces a secondary maximum in the phase lag spectrum corresponding to the outer edge of the disk. It could be responsible for the break in the time-lag Fourier spectrum observed in GBHs (see Fig. 6a).

Reflection is most probably not the main mechanism producing lags in GBHs, otherwise their energy dependence would be the same as that of the reflection albedo having local maximum around Fe Kα line (not observed). The reflection, however, *is* observed in the spectra of GBHs and therefore it must have an impact onto the timing properties. Determining the fraction of time lags produced by reflection is a matter of future work.

SUMMARY

There are several competing models for the X-ray production in accreting black holes (see Beloborodov, this volume). Most of these models make a number of ad hoc assumptions that are difficult to check. Temporal variability provides independent tests for the models. Already now there are a number of important consequencies from comparing model prediction to the data. For example, the mysterious hard time lags cannot result only from light travel effects in the Comptonizing cloud. In that case, the ACF's width would increase with photon energy which is opposite to the observed behavior. Strong constraints on the temporal behavior of the energy dissipation rate in flares can be obtained from the average shot profiles, CCFs, and the Fourier-frequency dependent lags. Most of the models concentrate on the properties of the Comptonizing radiation, while the Compton reflection can (and should) have a strong impact on the observed variability properties as shown here.

Unfortunately, basically all the models that are designed to explain temporal characteristics are still phenomenological and they are often based (as spectral models) on a number of questionable assumptions. We are making the first steps in designing a model that would be able (at least) not to contradict the observational facts. Concluding, I just would like to point out that real objects (such as Cyg X-1, for example) are very complex. Thus one can hardly expect that a model that satisfies the observational facts should be very simple.

ACKNOWLEDGEMENTS

This research was supported by the Swedish Natural Science Research Council and the Anna-Greta and Holger Crafoord Fund.

REFERENCES

Beloborodov, A. M., Plasma Ejection from Magnetic Flares and the X-ray Spectrum of Cygnus X-1, *ApJ*, **510**, L123-L126, 1999a.

Beloborodov, A. M., Accretion Disk Models, in High Energy Processes in Accreting Black Holes, eds. J. Poutanen and R. Svensson, ASP Conf. Series Vol. 161, pp. 295-314, ASP, San Francisco, 1999b (astro-ph/9901108).

Böttcher, M., and Liang, E. P., Comptonization Signatures in the Rapid Aperiodic Variability of Galactic Black Hole Candidates, *ApJ*, **506**, 281-288, 1998.

Böttcher, M., and Liang, E. P., A New Model for the Hard Time Lags in Black Hole X-ray Binaries, *ApJ*, **511**, L37-L40, 1999.

Churazov, E., Gilfanov, M., and Revnivtsev, M., Soft State of Cygnus X-1: Stable Disk and Unstable Corona, *MNRAS*, in press, 2001 (astro-ph/0006227).

Coppi, P. S., The Physics of Hybrid Thermal/Non-Thermal Plasmas, in High Energy Processes in Accreting Black Holes, eds. J. Poutanen and R. Svensson, ASP Conf. Series Vol. 161, pp. 375-403, ASP, San Francisco, 1999 (astro-ph/9903158).

Cui, W., Phase Lags of Quasi-periodic Oscillations in Microquasar GRS 1915+105, *ApJ*, **524**, L59-L62, 1999.

Cui, W., Zhang, S.N., and Chen, W., Phase Lags and Coherence Function of X-ray Emission from Black Hole Candidate XTE J1550-564, *ApJ*, **531**, L45-L48, 2000.

Cui, W., Zhang, S. N., Focke, W., and Swank, J. H., Temporal Properties of Cygnus X-1 During the Spectral Transitions, *ApJ*, **484**, 383-393, 1997.

Esin, A.A., Narayan, R., Cui, W., Grove, E.C., and Zhang, S.-N., Spectral Transitions in Cyg X-1 and Other Black Hole X-ray Binaries, *ApJ*, **505**, 854-868, 1998.

Feng, Y. X., Li, T. P., and Chen, L., X-Ray Shots of Cygnus X-1, *ApJ*, **514**, 373-382, 1999.

Gierliński, M., Zdziarski, A. A., Done, C., Johnson, W. N., Ebisawa, K., et al., Simultaneous X-ray and Gamma-ray Observations of Cyg X-1 in the Hard State by Ginga and OSSE, *MNRAS*, **288**, 958-964, 1997.

Gierliński, M., Zdziarski, A. A., Poutanen, J., Coppi, P. S., Ebisawa, K., Johnson, W. N., Radiation Mechanisms and Geometry of Cygnus X-1 in the Soft State, *MNRAS*, **309**, 496-512, 1999.

Gilfanov, M., Churazov, E., Sunyaev, R., Vikhlinin, A., Finoguenov, A., et al., Hard X-ray Observations of Black-Hole Candidates, in The Lives of the Neutron Stars, eds. M. A. Alpar, Ü. Kiziloglu, and J. van Paradijs, NATO C 450, pp. 331-354, Kluwer, Dordrecht,1995.

Gilfanov M., Churazov E., Revnivtsev M., 2000, Frequency-resolved Spectroscopy of Cyg X-1: Fast Variability of the Reflected Emission in the Soft State, *MNRAS*, **316**, 923-928, 2000.

Grebenev, S. A. Sunyaev, R., Pavlinsky, M., Churazov, E., Gilfanov, M., et al., Observations of Black Hole Candidates with GRANAT, *ApJS*, **97**, 281-287, 1993.

Grebenev, S. A., Sunyaev, R. A., and Pavlinsky, M. N., Spectral States of Galactic Black Hole Candidates: Results of Observations with ART-P/Granat, *Adv. Space Res.*, **19**, (1)15, 1997.

Grove, J. E., Johnson, W. N., Kroeger, R. A., McNaron-Brown, K., Skibo, J. G., Phlips, B. F., Gamma-Ray Spectral States of Galactic Black Hole Candidates, *ApJ*, **500**, 899-908, 1998a.

Grove, J. E., Strickman, M. S., Mats, S. M., Hua, X.-M., Kazanas, D., and Titarchuk, L. G., Timing Noise Properties of GRO J0422+32, *ApJ*, **502**, L45-L48, 1998b.

Haardt, F., Maraschi, L., and Ghisellini, G., A Model for the X-ray and UV Emission from Seyfert Galaxies and Galactic Black Holes, *ApJ*, **432**, L95-L99, 1994.

Hua, X.-M., Kazanas, D., and Cui, W., Probing the Structure of Accreting Compact Sources through X-ray Time Lags and Spectra, *ApJ*, **512**, 793-803, 1999.

Hynes, R. I., O'Brien, K., Horne, K., Chen, W., and Haswell, C. A., Echoes from an Irradiated Disc in GRO J1655-40, *MNRAS*, **299**, L37-L41, 1998.

Kato, S., Low-frequency, One-armed Corrugation Waves in Relativistic Accretion Disks, *PASJ*, **41**, 745-761, 1989.

Kazanas, D., Hua, X.-M., and Titarchuk, L., Temporal and Spectral Properties of Comptonized Radiation and its Application, *ApJ*, **480**, 735-740, 1997.

Lee, J. C., Fabian, A. C., Reynolds, C. S., Brandt, W. N., and Iwasawa, K., The X-ray Variability of the Seyfert 1 Galaxy MCG-6-30-15 from Long ASCA and RXTE Observations, *MNRAS*, **318**, 857-874, 2000.

Li, H., Kusunose, M., and Liang, E. P., Gamma Rays from Galactic Black Hole Candidates with Stochastic Particle Acceleration, *ApJ*, **460**, L29-L32, 1996.

Li, T. P., Feng, Y. X., and Chen, L., Temporal and Spectral Correlations of Cygnus X-1, *ApJ*, **521**, 789-797, 1999.

Lochner, J. C., Swank, J. H., and Szymkowiak, A. E., Shot Noise Parameters for Cygnus X-1 through Phase Portrait Fitting, *ApJ*, **376**, 295-211, 1991.

Maccarone, T. J., Coppi, P. S., and Poutanen, J., Time Domain Analysis of Variability in Cygnus X-1: Constraints on the Emission Models, *ApJ*, **537**, L107-L110, 2000.

Magdziarz, P., Blaes, O. M., Zdziarski, A. A., Johnson, W. N., and Smith, D. A., *MNRAS*, **301**, 179-192, 1998.

Malzac, J., and Jourdain, E., Temporal Properties of Flares in Accretion Disk Coronae, *A&A*, **359**, 843-854, 2000.

Malzac, J., Beloborodov, A. M., and Poutanen, J., X-ray Spectra of Accretion Discs with Dynamic Coronae, *MNRAS*, in press, 2001.

Mason, K. O., and Cordova, F. A., Infrared Photometry of the X-ray Binary 2A 1822-371 - A Model for the Ultraviolet, Optical, and Infrared Light Curve, *ApJ*, **262**, 253-262, 1982.

McConnell, M. L., Bennett, K., Bloemen, H.. Collmar, W., Hermsen, W., et al., The Spectral Variability of Cygnus X-1 at MeV Energies, in The Fifth Compton Symposium, eds. M. L. McConnell and J. M. Ryan, AIP Conf. Proc. Vol. 510, pp. 114-118, AIP, New York, 2000a (astro-ph/0001485).

McConnell, M. L., Ryan, J. M., Collmar, W., Schnfelder, V., Steinle, H., et al., A High-Sensitivity Measurement of the MeV Gamma-Ray Spectrum of Cygnus X-1, *ApJ*, **543**, 928-937, 2000b.

Misra, R., Modeling the X-Ray Timing Properties of Cygnus X-1 Caused by Waves Propagating in a Transition Disk, *ApJ*, **529**, L95-L98, 2000.

Miyamoto, S., and Kitamoto, S., X-ray Time Variations from Cygnus X-1 and Implications for the Accretion Process, *Nature*, **342**, 773-774, 1989.

Miyamoto, S., Kitamoto, S., Mitsuda, K., and Dotani, T., Delayed Hard X-rays from Cygnus X-1, *Nature*, **336**, 450-452, 1988.

Miyamoto, S., Kitamoto, S., Iga, S., Negoro, H., and Terada, K., Canonical Time Variations of X-rays from Black Hole Candidates in the Low-Intensity State, *ApJ*, **391**, L21-L24, 1992.

Negoro, H., Miyamoto, S., and Kitamoto, S., Structure of X-ray Shots of Cygnus X-1 in its Low State, *ApJ*, **423**, L127-L130, 1994.

Nolan, P L., Gruber, D. E., Matteson, J. L., Peterson, L. E., Rothschild, R. E., et al., Rapid Variability of 10-140 keV X-rays from Cygnus X-1, *ApJ*, **246**, 494-501, 1981.

Nowak, M. A., Vaughan, B. A., Wilms, J., Dove, J. B., and Begelman, M. C., Rossi X-ray Timing Explorer Observation Cygnus X-1. II. Timing Analysis, *ApJ*, **510**, 874-891, 1999a.

Nowak, M. A., Wilms, J., and Dove, J. B., Low-Luminosity States of the Black Hole Candidate GX 339-4. II. Timing Analysis, *ApJ*, **517**, 355-366, 1999b.

Nowak, M. A., Wilms, J., Vaughan, B. A., Dove, J. B., and Begelman, M. C., Rossi X-Ray Timing Explorer Observation of Cygnus X-1. III. Implications for Compton Corona and Advection-dominated Accretion Flow Models, *ApJ*, **515**, 726-737, 1999c.

Page, C. G., Study of Rapid Variability in Cygnus X-1, *Space Sci. Rev.*, 40, 387, 1985.

Papadakis, I. E., and Lawrence, A., A Detailed X-ray Variability Study of the Seyfert Galaxy NGC 4051, *MNRAS*, **272**, 161-183, 1995.

Payne, D. G., Time-dependent Comptonization: X-ray Reverberations, *ApJ*, **237**, 951-963, 1980.

Pottschmidt, K., Wilms, J., Nowak, M. A., Heindl, W. A., Smith, D. M., and Staubert, R., Temporal Evolution of X-ray Lags in Cygnus X-1, **357**, L17-L20, 2000.

Poutanen, J., Accretion Disc-Corona Models and X/γ-ray Spectra of Accreting Black Holes, in Theory of Black Hole Accretion Discs, eds. M. A. Abramowicz, G. Björnsson, J. E. Pringle, pp. 100-122, CUP, Cambridge, 1998 (astro-ph/9805025).

Poutanen, J., Time Lags in Compact Objects: Constraints on the Emission Models, in X-ray Astronomy 1999 - Stellar Endpoints, AGN and the Diffuse Background, eds. G. Malaguti, G. Palumbo, and N. White, Gordon & Breach, Singapore, in press, 2001 (astro-ph/0002505).

Poutanen, J., and Coppi, P. S., Unification of Spectral States of Accreting Black Holes, *Phys. Scripta*, **T77**, 57-59, 1998 (astro-ph/9711316).

Poutanen, J., and Fabian, A. C., Spectral Evolution of Magnetic Flares and Time Lags in Accreting Black Hole Sources, *MNRAS*, **306**, L31-L37, 1999.

Poutanen, J., and Svensson, R., The Two-Phase Pair Corona Model for Active Galactic Nuclei and X-ray Binaries: How to Obtain Exact Solutions, *ApJ*, **470**, 249-268, 1996.

Poutanen, J., Krolik, J. H., and Ryde, F., The Nature of Spectral Transitions in Accreting Black Holes - The Case of Cyg X-1, *MNRAS*, **292**, L21-L25, 1997.

Priedhorsky, W., Garmire, G. P., Rothschild, R., Boldt, E., Serlemitsos, P., and Holt, S., Extended-bandwidth X-ray Observations of Cygnus X-1, *ApJ*, **233**, 350-363, 1979.

Reig, P., Belloni, T., van der Klis, M., Mendez, M., Kylafis, N. D., and Ford, E. C., Phase Lag Variability Associated with the 1-10 Hz QPO in GRS 1915+105, *ApJ*, **541**, 883-888, 2000.

Smith, I. A., and Liang, E. P., Multiwavelength Observations of GX 339-4 in 1996. II. Rapid X-ray Variability, *ApJ*, **519**, 771-778, 1999.

Stern, B. E., Poutanen, J., Svensson, R., Sikora, M., and Begelman, M. C., On the Geometry of the X-ray Emitting Region in Seyfert Galaxies, *ApJ*, **449**, L13-L17, 1995.

Stern, B. E., Poutanen, J., and Svensson, R., Brightness-Dependent Properties of Gamma-Ray Bursts, *ApJ*, **489**, L41-L45, 1997.

Stern, B. E., Poutanen, J., and Svensson, R., A Complexity-Brightness Correlation in Gamma-Ray Bursts, *ApJ*, **510**, 312-324, 1999.

Sunyaev, R. A., and Titarchuk, L. G., Comptonization of X-rays in Plasma Clouds. Typical Radiation Spectra, *A&A*, **86**, 121-138, 1980.

Sutherland, P. G., Weisskopf, M. C., and Kahn, S. M., Short-term Time Variability of Cygnus X-1. II., *ApJ*, **219**, 1029-1037, 1978.

Terrell, N. J. Jr., Shot Noise Character of Cygnus X-1 Pulsations, *ApJ*, **174**, L35-L41, 1972.

Verbunt, F., Observations of Accretion Disks in X-ray Binaries, in Astrophysical Discs: An EC Summer School, eds. J. A. Sellwood and J. Goodman, ASP Conf. Series Vol. 160, pp. 21-32, ASP, San Francisco, 1999 (astro-ph/9809028).

Vikhlinin, A., A Method of Mass Measurement in Black Hole Binaries using Timing and High-Resolution X-Ray Spectroscopy, *ApJ*, **521**, L45-L48, 1999.

Vrtilek, S. D., Raymond, J. C., Garcia, M. R., Verbunt, F., Hasinger, G., and Kurster, M., Observations of Cygnus X-2 with IUE - Ultraviolet Results from a Multiwavelength Campaign, *A&A*, **235**, 162-173, 1990.

Weisskopf, M. C., Kahn, S. M., and Sutherland, P. G., Short-term Time Variability of Cygnus X-1, *ApJ*, **199**, L147-L151, 1975.

White, N. E., and Holt, S. S., Accretion Disk Coronae, *ApJ*, **257**, 318-337, 1982.

Zdziarski, A. A., X-rays and Soft Gamma-Rays from Seyferts, Radio Galaxies, and Black Hole Binaries, in High Energy Processes in Accreting Black Holes, eds. J. Poutanen and R. Svensson, ASP Conf. Series Vol. 161, pp. 16-35, ASP, San Francisco, 1999 (astro-ph/9812449).

Zdziarski, A. A., Johnson, W. N., and Magdziarz, P., Broad-band Gamma-ray and X-ray Spectra of NGC 4151 and Their Implications for Physical Processes and Geometry, *MNRAS*, **283**, 193-206, 1996.

Zdziarski, A. A., Johnson, W. N., Poutanen, J., Magdziarz, P., and Gierliński, M., X-rays and Gamma-Rays from Accretion Flows onto Black Holes in Seyferts and X-ray Binaries, in The Transparent Universe, ESA SP-382, pp. 373-380, 1997.

Zdziarski, A. A., Poutanen, J., and Johnson, W. N., Observations of Seyfert Galaxies by OSSE and Parameters of Their X-Ray/Gamma-Ray Sources, *ApJ*, **542**, 703-709, 2000.